Journal of Research and Applications in Mechanical Engineering
ISSN: 2229-2152 (Print); 2697-424x (Online)
(2025) Vol. 13, No. 3, Paper No. JRAME 25-13-047
[DOI: 10.14456/jrame.2025.47]

Research Article

Effect of Tube Ice Thickness on Energy Consumption in Tube Ice Production Using Thermodynamic Model

K. Phanwor
T. Pornpibul*
School of Mechanical Engineering, Institute of Engineering, Suranaree University of Technology, Nakhon Ratchasima, 30000, Thailand

Received 7 September 2024
Revised 3 November 2024
Accepted 21 November 2024

Abstract:
This research article analyzes the effect of tube ice thickness on duration and energy consumption in the freezing process for tube ice production, employing thermodynamic models based on mass and energy balance principles. Thermal simulations using the successive substitution method were calculated in MATLAB, demonstrating a 3.75% error compared to the actual process. The results show that the freezing duration varies with the required ice thickness. In addition, ice thickness significantly influences specific heat energy consumption (SEC_H) and specific electrical energy consumption (SEC_E). The case study reveals that as ice thickness increases, SEC_H rises due to the thermal insulation properties of the ice, which impedes heat transfer and slows ice formation. This results in a decreased cooling load and, consequently, a reduction in electrical energy efficiency. However, when the ice thickness reaches 12.24 mm, the rate of thickness formation accelerates, indicating an improvement in electrical energy efficiency. The study concludes that SEC_E is a critical parameter that reflects the combined effect of the average electrical energy consumption rate and the ice formation thickness rate, thus representing the characteristics of the ice-making machine. These findings provide a basis for optimizing electrical energy efficiency by controlling ice thickness, with potential implications for cost savings and enhanced sustainability in tube ice production.

Keywords: *Thermodynamic model, Tube ice production, Freezing process, Tube ice thickness, Energy consumption*

1. Introduction

Thailand's hot and humid climate creates a high demand for ice, especially tube and crushed ice for beverages, and block ice for food preservation. Notable, electricity consumption makes up the primary cost of ice production. Moreover, a study [1] shows that tube ice production is the most energy-efficient, while crushed ice production uses 4.3% more electricity. Block ice production uses 51.8% more electricity than tube ice. Consequently, tube ice has become the most widely used. It has a cylindrical shape with a hollow center along its length, as shown in Fig. 1.

Tube ice production involves 4 stages: 1) the water-feeding process, 2) the freezing process, 3) the defrosting process, and 4) the cutting process. The freezing stage is time-consuming and has the highest electricity consumption rate [1]. Subsequently, experimental studies [2, 3] were conducted to examine the rate of tube ice formation. The results indicate that ice forms rapidly at first but slows down over time. As a thermal insulator, the ice thickness resists heat transfer to the refrigerant. Therefore, ice thickness impacts production time and energy consumption during tube ice production.

* Corresponding author: T. Pornpibul
E-mail address: Teeracha@sut.ac.th

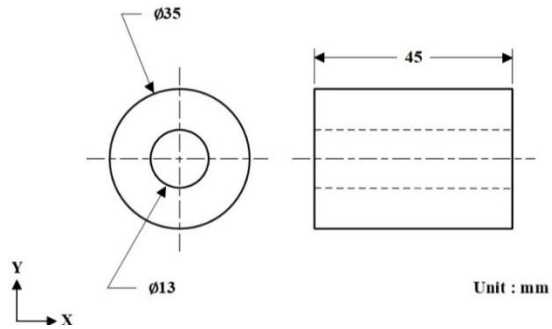

Fig. 1. Dimension of a tube ice.

A study [4] investigates production time and specific heat energy consumption (SEC_H) during the freezing process. The results show that during the first 14 minutes, ice forms rapidly, and heat transfer decreases continuously. This effect causes a decrease in SEC_H, which is an advantage for tube ice production. However, SEC_H increases due to thermal insulation from the ice thickness. This resists heat transfer and ice formation as the freezing process continues until it is completed in 28 minutes. Therefore, the study on tube ice production focuses on increasing the ice formation rate to decrease process time. A study [5] finds that using roughened tubes decreases production time compared to smooth tubes. Another study [6] shows that adding fins decreases freezing time and energy use by up to 13%. Moreover, a study [7] finds that smaller tubes enable faster ice formation and lower energy consumption compared to larger tubes. In addition, studies [8, 9] show that installing pre-cooling equipment for feed water reduces both production time and electricity consumption.

Literature reviews indicate that improving tube ice production efficiency mainly focuses on decreasing process time to reduce electricity consumption. However, the ice formation rate continues to decrease as the ice layer thickness increases, causing the freezing process to extend in duration. In addition, tube ice production does not account for the ratio of electrical energy consumption to ice thickness formation during the freezing process, which this study represents using specific electrical energy consumption (SEC_E). This parameter is important for tube ice production because SEC_E shows the characteristics of electrical energy consumption for ice thickness formation during the freezing process. Furthermore, numerical methods and heat equation modeling are used to predict freezing process time, ice formation rate, and cooling load to assess heat energy efficiency [4-7, 10]. These methods do not account for mass transfer or changes in water temperature, causing simulation results to differ from experimental data. This study uses a thermodynamic model that includes mass, heat, and work transfer to achieve more realistic results. It also considers decreasing the water temperature before ice formation to better estimate study factors such as freezing process time, SEC_H, SEC_E, and changes in ice thickness during the process.

Therefore, the objective of this article is to analyze the effects of ice thickness on freezing time and energy consumption in tube ice production. The analysis uses a thermodynamic model based on mass and energy balance, combined with a successive substitution method for system simulation.

2. Freezing process in tube ice production

Tube ice production involves four main processes: 1st the water-feeding process, water is fed into the tube ice freezer tower. 2nd the freezing process, the water freezes into tube ice of the required thickness using a vapor compression cycle. 3rd the defrosting process, the ice is slightly melted to release it from the tubes. Finally, the cutting process, the ice is cut to the desired length. These steps, which operate using the tube ice-making machine, are shown in Fig. 2.

The freezing process occurs in the freezer tower at atmospheric pressure. Ammonia (NH_3) is used as the refrigerant. The simulation is divided into two phases, each having different heat transfer characteristics:

1) Chilling water phase: In this phase, the refrigeration system cools the feed water to 0°C.
2) Ice-making phase: The phase entails the solidification of tube ice until the required ice thickness is achieved.

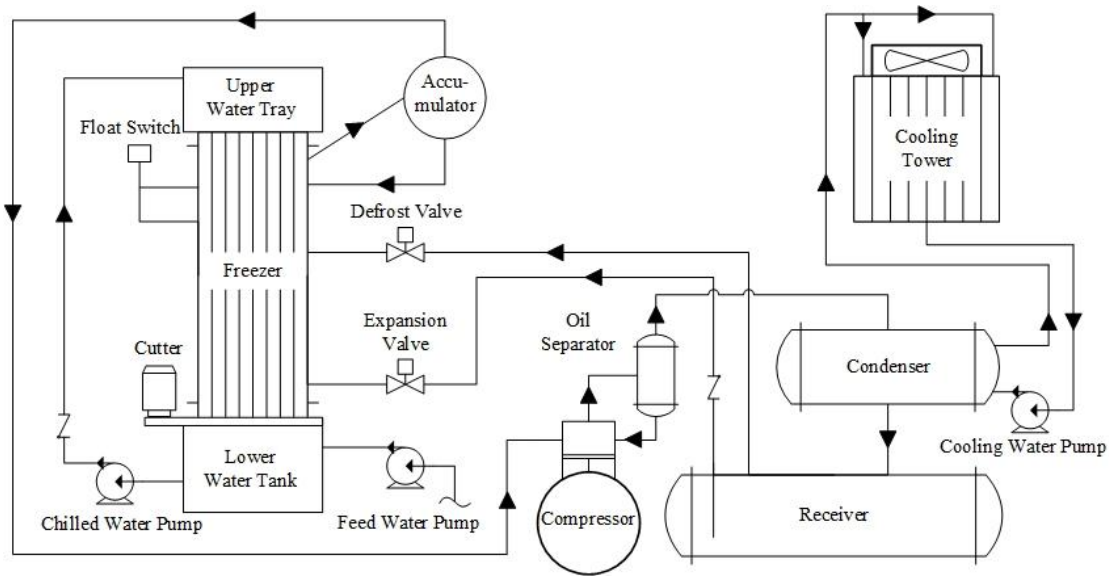

Fig. 2. Schematic of tube ice-making machine.

3. Thermodynamic models

The thermodynamic model used in this research is based on the 1st law of thermodynamics [11], applying mass and energy balance principles, as illustrated in Eqs. (1) and (2) respectively.

$$\sum m_{in} - \sum m_{in} = \Delta m_{sys} \tag{1}$$

$$\sum E_{in} - \sum E_{out} = \Delta E_{sys} \tag{2}$$

The freezing process is classified as an unsteady-state process ($\Delta E_{sys} \neq 0$). This classification describes both steady-state and unsteady-state processes. Below are examples of thermodynamic model applications from various studies:

Steady-State Process ($\Delta E_{sys}=0$): This type of process occurs when the energy or state of the system remains constant over time. It is observed in systems where the properties of the substances within the control volume or equipment remain constant. For example, in the boiling and heating process of sugarcane juice, the assumption is steady-state conditions because the state of the juice in the boiler and heater remains the same over time. In a study [12], a thermodynamic model predicts the steam consumption of the boiler and heater, with only a 5% error compared to the actual process. A study [13] develops a new method to measure the heat generated by battery cells, focusing on reducing heat loss to the surrounding environment. This method uses an energy balance model that accurately predicts heat production. It can be used to design effective thermal management systems for battery packs.

Unsteady-State Process ($\Delta E_{sys} \neq 0$): This process involves changes in the system's energy or state over time, occurring when the properties of the substances inside the control volume or equipment change. An example is the sterilization process in canned fruit production. In this process, unsterilized fruit is placed in cans and input into a sterilizer. Steam at 120°C is injected into the sterilizer, resulting in changes in the state of both the canned fruit and the steam during the process. A study [14] uses a thermodynamic model to predict the steam consumption rate and temperature during sterilization. The model shows accurate predictions for the steam consumption ratio, with only a 1–2°C error in the predicted steam temperature compared to the average steam consumption. In addition, the hydrogen injection process into storage tanks for fuel cell electric vehicles (FCEV) is an unsteady-state process because of pressure and temperature changes during filling. In a study [15], a thermodynamic model predicts the pressure, temperature, and filling time of hydrogen in the storage tank. The model's predictions for hydrogen filling time have a 3% margin of error compared to the experimental data.

The analysis examines the effect of tube ice thickness on energy consumption during the freezing process. A thermodynamic model is suitable for predicting the cooling load (kW), the rate of ice formation (kg/s), and the rate of ice thickness formation (mm/s). The electrical energy consumption rate (kW) is measurement data from the actual process in a study [16]. This data reflects the electrical energy consumption of the compressor. Meanwhile, the cooling load, mass ice formation rate, and thickness of ice formation are predicted using a system simulation based on a thermodynamic model. This model focuses on four main devices: the freezer tower, ice tubes, shell-and-tube heat exchanger, and lower water tank. These parameters cannot be directly measured and require permission from the owner to measure the ice formation rate to avoid contaminating the ice with pathogens.

3.1 Tube ice freezer tower

Designs a mass control system for a closed system that observes water in the freezer tower, as illustrated in Fig. 3.

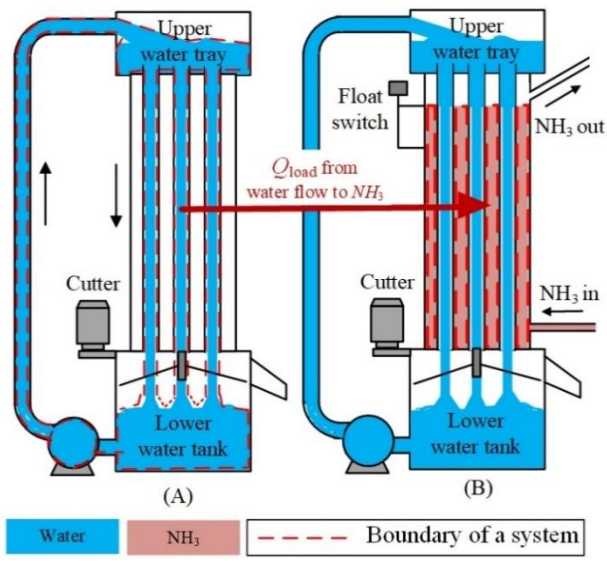

Fig. 3. Control mass of freezer tower: (A) Water system (B) Liquid NH_3 system.

The temperature change of the chilled water during the chilling water phase is analyzed using the energy balance shown in Eq. (2) for the control volume in Fig. 3(A). This phase represents an unsteady state in the system, caused by changes in water temperature as heat transfers from the water to NH_3. The model is presented in Eq. (3):

$$T_{w,t+\Delta t} = T_{w,t} - \left[\left(\sum_{j=1}^{n} \dot{Q}_{Load}^{j} \cdot \Delta t\right) \Big/ \left(m_{w,sys} c_{p,w}\right)\right] \tag{3}$$

The mass of ice formed during the ice-making phase is analyzed using the energy balance in Eq. (2) for the control volume shown in Fig. 3(A). This phase represents an unsteady state in the system as water changes into tube ice. Heat transfers from the water through the ice and the tube to NH_3. The model is presented in Eq. (4):

$$\sum_{j=1}^{n} \Delta m_i^j = \left[\left(\sum_{j=1}^{n} \dot{Q}_{Load}^{j} \cdot \Delta t\right) \Big/ \left(u_w - u_i\right)\right] \tag{4}$$

The thickness of the tube ice is determined using the mass balance in Eq. (2) for the control volume in Fig. 3(A), which predicts the mass of ice based on Eq. (4). The thickness calculation considers the shape of the ice-making tube. The model is presented in Eq. (5):

$$\Delta r_i = \sqrt{\left(\sum_{j=1}^{n} \Delta m_i^j\right) \Big/ \left(\rho_i \pi z_i\right)} \tag{5}$$

The evaporation rate of the refrigerant during the freezing process is determined using the energy balance in Eq. (2) for the control volume shown in Fig. 3(B). This system operates under steady-state conditions, meaning there are no energy changes as the refrigerant level remains constant while heat is added, causing evaporation at a saturated temperature. The model is presented in Eq. (6):

$$\dot{m}_{evap} = \sum_{j=1}^{n} \dot{Q}_{Load}^{j} \Big/ (h_{fg}) \tag{6}$$

To predict the water temperature and the amount of ice formed in the freezer tower, it is important to know the heat transfer rate from the water through the ice-making tube to the NH_3 (cooling load). This heat transfer occurs around the ice-making tube, so we need to develop a model for the ice-making tube in the next section.

3.2 Ice-making tube

Define a control volume within a tube to separate water and ice as a system, as illustrated in Fig. 4.

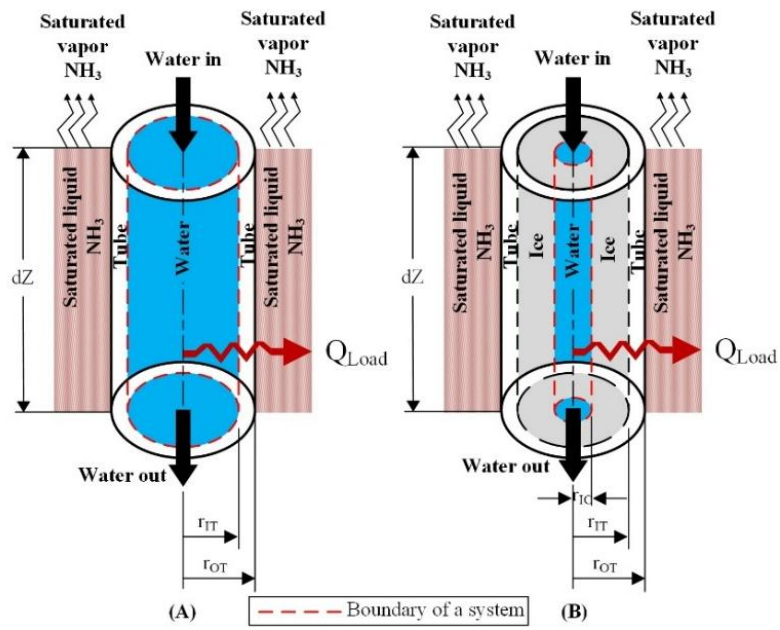

Fig. 4. Control volume of tube: (A) Water system (B) Water & ice system

The cooling load during the chilling water phase and the ice-making phase is shown in Eqs. (7) and (8), respectively. This model uses the energy balance explained in Eq. (2) for the control volume illustrated in Fig. 4. The cooling load is determined by the temperature difference between the water inside the tube and the refrigerant surrounding the ice-making tube. Consequently, the water continuously cools down until it freezes into ice at 0°C.

$$\dot{Q}_{Load}^{j} = \dot{m}_{w}^{j} \left[c_{p,w} \left(T_{w,in}^{j} - T_{w,out}^{j} \right) + \left(KP^{j} \right) \right] \tag{7}$$

$$\dot{Q}_{Load}^{j} = \frac{\Delta m_{i}^{j}}{\Delta t} \left[(u_{w} - u_{i}) + \frac{1}{2} \left(v_{w,out}^{j} \right)^{2} \right] + \dot{m}_{w,in}^{j} \left[KP^{j} \right] \tag{8}$$

The model that predicts the cooling load has some unknown variables. These include the inlet and outlet temperatures of the water flowing through the ice-making tube during the chilling water phase. The amount of ice formed in the ice-making tube during the ice-making phase is also unknown. Therefore, the next section discusses the model of the shell-and-tube heat exchanger.

3.3 Shell and tube heat exchanger

The freezer tower operates as a shell-and-tube heat exchanger, where heat transfers at a constant temperature of the cold fluid. Consequently, this model uses the overall heat transfer coefficient [17, 18]. Additionally, the model considers the tube section and the average temperature difference of the water during the chilling water phase. In the ice-making phase, the temperatures of both the water and the refrigerant are assumed to be constant. The cooling load models for the chilling water and ice-making phases are presented in Eqs. (9) and (10), respectively.

$$\dot{Q}_{Load}^{j} = UdA^{j}\left[\frac{1}{2}\left(T_{w,in}^{j} + T_{w,out}^{j}\right) - T_{NH_3}\right] \tag{9}$$

$$\dot{Q}_{Load}^{j} = UdA^{j}\left(T_{w} - T_{NH_3}\right) \tag{10}$$

Based on Eqs. (7) and (9), define a model to calculate the outlet water temperature of the tube section, as shown in Eq. (11). Moreover, Eqs. (8) and (10) define a model for the ice formed inside the tube, as shown in Eq. (12).

$$T_{w,out}^{j} = \left\{\left(\frac{1}{2}UdA^{j}\right) + \left(\frac{1}{\Delta t}m_{w}^{j}c_{p,w}\right)\right\}^{-1}\left\{\left[UdA^{j}\left(T_{NH_3} - \frac{T_{w,in}^{j}}{2}\right)\right] + \frac{m_{w}^{j}}{\Delta t}\left[\left(c_{p,w}T_{w,in}^{j}\right) + \left(KP^{j}\right)\right]\right\} \tag{11}$$

$$\Delta m_{i}^{j} = \left[UdA^{j}\left(T_{w} - T_{NH_3}\right)\Delta t - m_{w,in}^{j}\left(KP^{j}\right)\right] \Big/ \left[\left(u_{w} - u_{i}\right) + \left(\frac{1}{2}\left(v_{w,out}^{j}\right)^{2}\right)\right] \tag{12}$$

The overall heat transfer coefficient during the chilling water phase includes the thermal resistances of the water, tube, and NH_3 [19]. In the ice-making phase, the thermal resistances consist of those of the water, ice, tube, and NH_3 [20]. These are presented in Eqs. (13) and (14), respectively.

$$UdA = \frac{1}{\left(R_{w} + R_{Tube} + R_{NH_3}\right)} \tag{13}$$

$$UdA = \frac{1}{\left(R_{w} + R_{i} + R_{Tube} + R_{NH_3}\right)} \tag{14}$$

The duration of the freezing process for both the chilling water phase and the ice-making phase is determined by the changing conditions of the water in the lower water tank.

3.4 Lower water tank

Define a control volume within a lower water tank, as illustrated in Fig. 5.

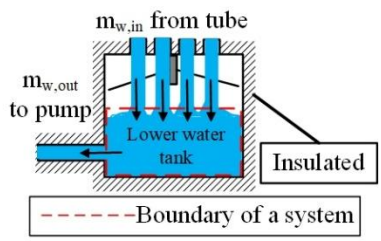

Fig. 5. Control volume of water in the lower tank.

The duration of the freezing process is divided into two phases: the chilling water phase, which considers the changing water temperature in the lower water tank, and the ice-making phase, which focuses on the decrease in water mass within the lower tank. Apply the energy balance in Eq. (2) for the control volume in Fig. 5. These are presented in Eqs. (15) and (16), respectively.

$$\Delta t = \left[\frac{m_{w,tank} c_{p,w} \left(T_{w,t+\Delta t} - T_{w,t} \right)}{\dot{m}_w c_{p,w} \left(T_{w,in} - T_{w,out} \right)} \right] \tag{15}$$

$$\Delta t = \left[u_w \left(\sum_{j=1}^{n} \Delta m_i^j \right) \Big/ h_w \left(\dot{m}_{w,in} - \dot{m}_{w,out} \right) \right] \tag{16}$$

4. Thermal simulations for the freezing process

4.1 Classification of variables

According to the thermodynamic model of thermal equipment, the variables are divided into three groups, as illustrated in Fig. 6.

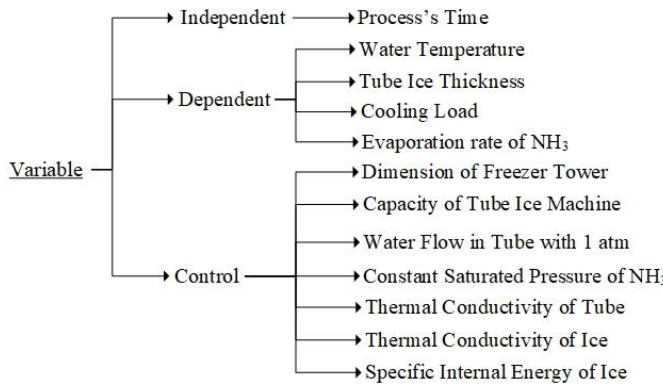

Fig. 6. System simulation variable classification diagram

4.2 System of equation

The analysis of thermal equipment for creating a thermodynamic model aims to predict important parameters such as freezing time, cooling load, refrigerant evaporation rate, and tube ice thickness. These models are presented in a system of equations in Table 1.

Table 1: Equation system in a freezing process.

Chilling water phase			**Ice-making phase**		
Function	Equation	Relation	Function	Equation	Relation
f_1	(13)	$f_1 = f\left(T_{w,in}^j, T_{NH_3}\right)$	F_1	(14)	$F_1^j = f\left(r_{IC,t}^j\right)$
f_2	(11)	$f_2^j = f\left(f_1^j, \Delta t, T_{w,out}^{j-1}\right)$	F_2	(12)	$F_2^j = f\left(F_1^j, \Delta t\right)$
f_3	(7)	$f_3^j = f\left(f_2^j, T_{w,out}^{j-1}\right)$	F_3	(8)	$F_3^j = f\left(F_2^j\right)$
f_4	(3)	$f_4 = f\left(f_3^{j=1\to n}\right)$	F_4	(4)	$F_4 = f\left(F_3^{j=1\to n}\right)$
f_5	(15)	$f_5 = f\left(f_2^n, f_4\right)$	F_5	(5)	$F_5 = f\left(F_4\right)$
f_6	(6)	$f_6 = f\left(f_3^{j=1\to n}\right)$	F_6	(16)	$F_6 = f\left(F_4\right)$
			F_7	(6)	$F_7 = f\left(F_3^{j=1\to n}\right)$

4.3 Successive substitution method

Thermal system simulations can be divided into three methods: 1) Sequential Substitution: In this method, the output from each equation serves as the input for the next one. This approach requires a clear flow diagram and proper sequencing of equations. However, it is unsuitable for unsteady-state processes because the independent variables change continuously. 2) The Newton-Raphson Method: This method quickly converges to a solution but may diverge

in systems with exponential functions, making it unsuitable for unsteady-state processes where independent variables change. 3) The Successive Substitution Method: The process begins with an initial approximation for the independent variables. These values are then substituted into equations to produce new results. This iterative process continues until the values are constant. It is suitable for unsteady-state processes. An information flow diagram is necessary for this method [21]. Consequently, the Successive Substitution Method is suitable for the freezing process, which is an unsteady-state process where independent variables change. An information flow diagram for the freezing process is illustrated in Fig. 7.

MATLAB [22] is used to solve the system of equations, with COOLPROP, an open-source software, providing thermodynamic properties specifically for pure substances such as water and NH_3 in this study. For studies that require thermodynamic properties of mixtures, such as for selecting suitable mixtures under specific process conditions [23], REFPROP is recommended. This commercial software offers accurate predictions of thermodynamic properties for mixtures.

4.4 Data of simulation

Case Study: The freezing process simulation uses data from a tube ice-making machine with a capacity of 50 tons/day, including data on the average compressor energy consumption rate and production conditions from [16]. This system operates with a freezing process time of 36 minutes and produces tube ice with a thickness of 12.33 mm, as presented in Table 2. Additionally, the validation of the simulation uses both the ice thickness measurements [16] and the results of previous simulations based on the mathematical model [10].

Table 2: Data of simulation.

	Parameter	**Value**	**Unit**
Control variable	Outer diameter of tubes	41	mm
	Inner diameter of tubes	35	mm
	Tube length	3.5	m
	Ice length	3	m
	Tube quantity	540	Tube
	Electrical energy consumption rate (compressor)	125	kW
	Evaporation refrigerant temperature	-10.9	ºC
	Ice density	910	kg/m^3
	Ice thermal conductivity	2.22	W/mºC
	Tube thermal conductivity	15.09	W/mºC
	Tube ice thickness required	12.33	mm
Initial condition	Feed water temperature	27.5	ºC
	Tube ice thickness	0	mm

5. Analysis of specific energy consumption for the freezing process

5.1 Specific heat energy consumption

Specific heat energy consumption (SEC_H) is calculated by considering the cooling load during the ice-making phase and the rate of ice formation, as presented in Eq. (17). SEC_H is used to describe the effects of two important parameters in the freezing process: the cooling load and ice formation rate. An increase in SEC_H indicates a lower ice formation rate due to the thermal insulation of the ice layer. This effect decreases the cooling load in the freezing process. However, a decrease in SEC_H demonstrates a higher ice formation rate due to the thin ice layer in the initial ice-making phase. This effect increases energy efficiency in the freezing process.

$$SEC_H = \frac{\dot{Q}_{load}}{\dot{m}_i} \tag{17}$$

5.2 Specific electric energy consumption

In this study, specific electrical energy consumption (SEC_E) is the inverse of electrical energy efficiency. This factor indicates the characteristics of two important parameters in the freezing process: the electrical energy consumption rate and the ice formation thickness rate, as presented in Eq. (18). An increase in SEC_E demonstrates a lower rate of

ice thickness formation while the average electrical energy consumption rate remains constant. However, a decrease in SEC_E shows a higher rate of ice thickness formation, while the average electrical energy consumption rate remains constant.

$$SEC_E = \frac{E_E}{3600\Delta\dot{r}_i} \tag{18}$$

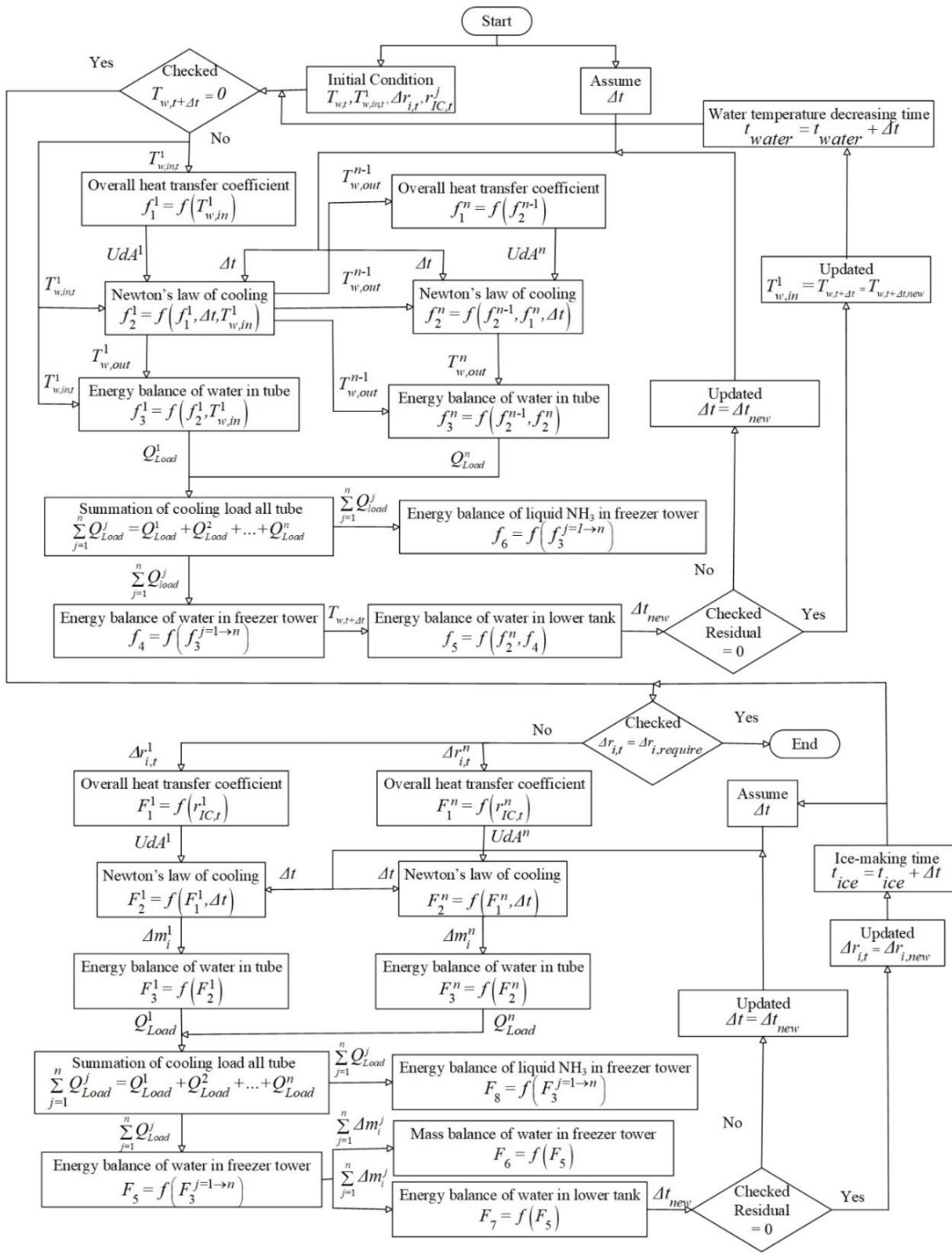

Fig. 7. Information flow diagram of a freezing process by successive substitution.

6. Results and Discussion

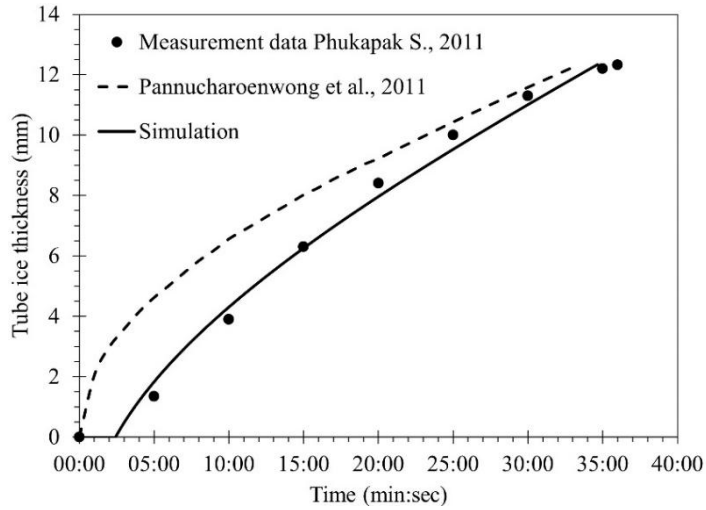

Fig. 8. Validation of simulation.

The validation of the simulation in Fig. 8 confirms that the simulation is accurate, based on actual production conditions [16]. The actual production takes 36 minutes to produce tube ice with a thickness of 12.33 mm. The simulation predicts a freezing time of 34 minutes and 39 seconds, representing a 3.75% error compared to the actual process. In contrast, the simulation [10] predicts a freezing time of 33 minutes and 25 seconds, resulting in a 7.18% error. This demonstrates the advantage of using a thermodynamic model: it can decrease the error in freezing process time predictions by 3.43%. This improvement results from the thermodynamic model's focus on the energy transfer of the water flowing in the tube during the freezing process, and the chilling water phase is important in the initial stage of the freezing process. This concept eliminates gaps and improves the limitations of the models in previous research. In addition, the simulation results indicate that the thickness of the tube ice increases over time, but the rate of ice formation decreases because of the thermal resistance of the ice layer. This rate of tube ice formation contributes to the analysis of SEC_H and SEC_E, respectively.

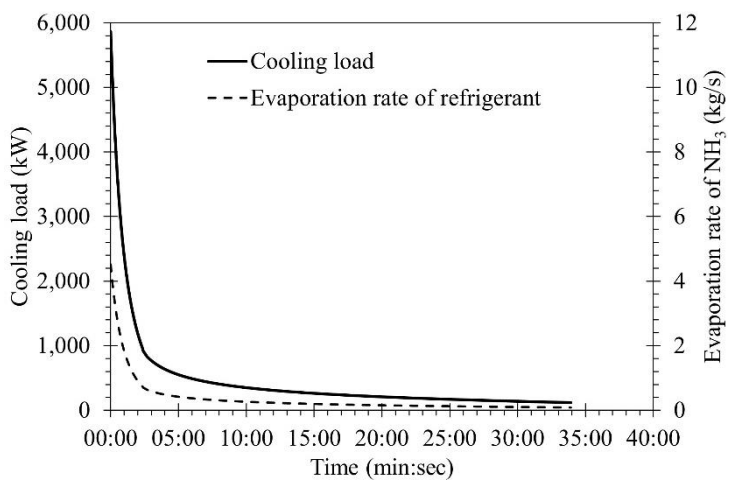

Fig. 9. Cooling load and evaporation rate of NH_3 throughout the process.

The freezing process of water in the freezer tower operates under the assumption that the refrigerant temperature remains constant. Therefore, during the chilling water phase, the cooling load depends on the changing water temperature, as shown in Fig. 9. The water temperature is highest at the beginning of the process, resulting in the maximum cooling load. As refrigeration continues, the water temperature drops, reducing the cooling load until the

water reaches 0°C and becomes ready to freeze. This occurs 2 minutes and 41 seconds before the ice-making phase begins. Previous studies [4, 5, 7, 24] do not account for the drop in water temperature in the freezer tower before the ice-making phase. This elimination directly affects the cooling load during the chilling water phase. Consequently, the predicted cooling load from these previous studies may be inconsistent with the actual process.

The ice-making phase has a lower cooling load than the chilling water phase. The cooling load decreases over the ice-making time, as shown in Fig. 9. The assumption is that the ice formation at a constant temperature of 0°C, resulting in a stable temperature difference between the water and the refrigerant. Therefore, the decrease in the cooling load is affected by the ice thickness layer insulator. The specific energy required for this formation is a constant 333.24 kJ/kg during this phase. The cooling load depends on the mass of the water phase change to ice. In addition, the assumption is that the refrigerant evaporates at a constant evaporation pressure, so the refrigerant evaporation rate is consistent with the cooling load. The cooling load is important for determining SEC_H.

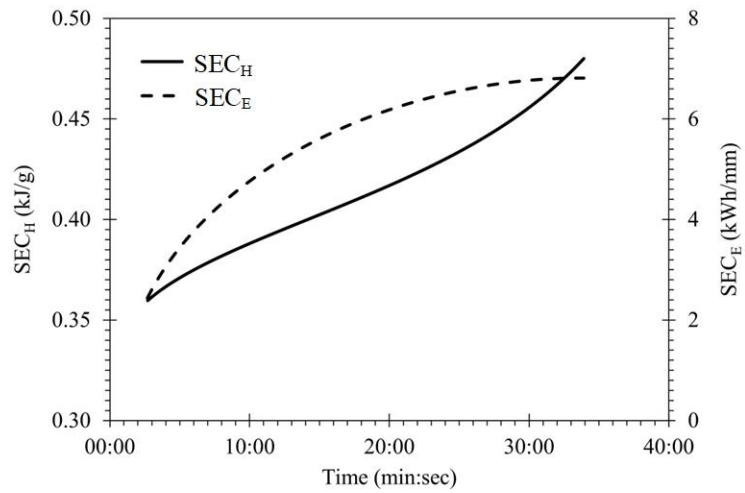

Fig. 10. SEC_H and SEC_E throughout the ice-making process.

The cooling load and the rate of ice formation continuously cause SEC_H to increase until the end of the process, as illustrated in Fig. 10. SEC_H significantly increases after 14 minutes and 20 seconds (ice thickness of 5.92 mm). This result is consistent with the findings of [4, 6, 7]. This study also confirms that the increase in SEC_H results from the thermal insulation effect of the tube ice thickness. This effect resists heat transfer and slows the rate of ice formation, resulting in a decrease in the cooling load. The previous study focuses on improving heat transfer in tube ice production. This improvement is modifications to the external tube surface with a rough coating [5] and wavy fins [6]. These improvements support more heat transfer during tube ice formation, resulting in a decrease in SEC_H.

The rate of tube ice thickness formation and the average electrical energy consumption affect SEC_E, as illustrated in Fig. 10. This represents a new finding in this research: SEC_E is the inverse of electrical energy efficiency. Thickness formation rates of ice decrease while the average electrical energy consumption remains stable throughout the freezing process. This result indicates a loss of electrical energy efficiency. However, when the freezing duration reaches 33 minutes and 38 seconds (with a tube ice thickness of 12.24 mm), the rate of thickness formation increases because ice forms in a smaller diameter. This finding indicates an increase in electrical energy efficiency. The SEC_E is an important parameter that reflects the combined effect of the average electrical energy consumption rate and the ice formation thickness rate. Therefore, SEC_E represents the characteristics of this ice-making machine. Furthermore, SEC_E has another advantage in this study; it allows manufacturers or owners to estimate their electricity costs for producing ice at various thicknesses.

7. Conclusion

This study analyzes the effect of tube ice thickness on duration and energy consumption during the freezing process of tube ice production. It uses thermodynamic models based on mass and energy balance principles. The system simulation uses successive substitution methods. The validation of the simulation represents a 3.75% error compared

to the actual process. The findings indicate that the thickness of the tube ice affects the freezing duration. As the required thickness increases, the duration also increases. Moreover, the ice formation rate decreases because of the thermal insulation provided by the ice thickness. The thickness of the tube ice directly affects both SEC_H and SEC_E. The case study shows that SEC_H increases throughout the process mainly because of thermal insulation of the thickness of the tube ice, which resists heat transfer and slows the rate of ice formation. This result decreases the cooling load throughout the process. In addition, the electrical energy consumption rate tends to remain stable. This effect demonstrates a decrease in electrical energy efficiency. However, when the ice thickness reaches 12.24 mm, the rate of thickness formation increases because ice forms in a smaller diameter. This finding indicates an increase in electrical energy efficiency. In this study, SEC_E is the inverse of electrical energy efficiency. SEC_E is an important parameter that reflects the combined effect of the average electrical energy consumption rate and the ice formation thickness rate. Therefore, SEC_E represents the characteristics of this ice-making machine.

The findings of this study can be applied in the industrial sector. The developed model accurately predicts the freezing duration needed to produce tube ice of varying thickness, allowing manufacturers to fine-tune machine timers with greater precision. Furthermore, the SEC_E concept supports accurate cost estimation for the freezing process per production cycle at different ice thicknesses. This concept enables more efficient production planning and cost management.

8. Future Work

Future work for tube ice production to improve energy consumption efficiency and model development includes four topics: 1) Implementing a pre-cooling system for the feed water conditions the water to be as close to freezing as possible before it enters the freezer tower. This approach can increase the ice formation rate and enhance the electrical energy efficiency. 2) Enhancing electrical energy efficiency can focus on reducing the power consumption of compressors and pumps with motor-driven equipment. This involves implementing a Variable Speed Drive (VSD) system. 3) Include energy consumption data from equipment involved in the freezing process, such as the chilled water pump, feed water pump, cooling water pump, and cooling tower fan, to improve the SEC_E calculation. And 4) Model development considers the simultaneous chilling water and ice-making phases in the freezer tower. The assumption is that water in contact with the tube surface rapidly heat transfer and freezes, while the adjacent water layers gradually transfer heat and decrease in temperature.

Acknowledgments

Thank you to Kitti Bundit scholarships, Suranaree University of Technology for granting scholarships for research work.

Nomenclature

c_p	[J/kg ºC]	Specific heat capacity
dA	[m^2]	Sub-section area of tube
E	[kJ]	Energy
h	[kJ/kg]	Enthalpy
KP	[kJ/kg]	Summation of specific kinetic energy and potential energy
m	[kg]	Mass
$\dot{m}$	[kg/s]	Mass flow rate
$\dot{Q}_{Load}$	[kW]	Cooling load
R	[ºC/W]	Thermal resistance
Δr	[m]	Thickness
$\Delta \dot{r}$	[m/s]	Thickness rate
T	[ºC]	Temperature
U	[W/m^2 ºC]	Overall heat transfer coefficient
u	[kJ/kg]	Internal energy
v	[m/s]	Velocity
z	[m]	Length

Greek symbols

α	[W/m^2 ºC]	Convective heat transfer coefficient
ρ	[kg/m^3]	Density

Subscripts and superscripts

j	[-]	Sub-section tube
n	[-]	Number of tubes
in	[-]	Inlet
out	[-]	Outlet
w	[-]	Water
i	[-]	Ice
NH_3	[-]	Ammonia
fg	[-]	Saturated liquid and vapor
$evap$	[-]	Evaporate
sys	[-]	System
E	[-]	Electrical
H	[-]	Heat
t	[sec]	Time
Δt	[sec]	Time difference

References

[1] Pornpibul T. A study of the cooling load in block-ice production and improving the ice production process for energy saving. IRTC. 2017.

[2] Pannucharoenwong N, Benchapiyaporn C, Ladsritha R, Thongyotee S. The study of parameters effect of solidification tubular ice. The Journal of Industrial Technology. 2013;9(3):63–80.

[3] Phukapak S, Benchapiyaporn C. Experimental study the parameter that affects solidification process of tube ice. In: Proceedings of The 25th Conference of the Mechanical Engineering Network of Thailand (ME-NETT 25); 2011; Krabi. Krabi: Kasetsart University; Thai Society of Mechanical Engineers. 2011.

[4] Tangthieng C. Effect of production time on energy use of a tube-ice making tower. Science & Technology Asia. 2010;15(2):1–9.

[5] Ghabkham P. A study to improve the tubular-ice production efficiency [Master's thesis]. Bangkok: Chulalongkorn University; 2004.

[6] Pannucharoenwong N, Saeng-uthai S, Promteerawong P, Benjapiyaporn C, Theerakulphisut S, Benjapiyaporn J. Experiment to enhance the efficiency of tubular ice production machine using the installation of wavy fin on ice making tube. Materials Today: Proceedings. 2017;4(5 Pt 2):6296–6305.

[7] Tangthieng C. Effect of tube diameter on the specific energy consumption of the ice making process. Applied Thermal Engineering. 2011;31(5):701–707.

[8] Pannucharoenwong N, Benjapiyaporn C, Theerakulpisut S, Saeng-Uthai S, Benjapiyaporn J, Promteerawong P. 50 ton tubular ice factory production optimization. Engineering and Applied Science Research. 2016;43:180–182.

[9] Pannucharoenwong N, Benjapiyaporn J, Benjapiyaporn C. An industrial utilization of tubular ice production facility towards energy optimization using the study of initial parameters in production. 2017.

[10] Pannucharoenwong N, Benchapiyaporn C, Benchapiyaporn J. A simulation of tubular-ice solidification with comparing numerical method in Cartesian and polar coordinates. In: Proceedings of The 25th Conference of the Mechanical Engineering Network of Thailand (ME-NETT 25); 2011; Krabi. Krabi: Kasetsart University; Thai Society of Mechanical Engineers. 2011.

[11] Borgnakke C, Sonntag RE. Fundamentals of thermodynamics. John Wiley & Sons; 2020.

[12] Klabklay T, Pornpibul T. Thermodynamics model of multiple boiling and heating in production sugar process. Journal of Science and Technology Mahasarakham University. 2013;32(5):606–616.

[13] Kulranut J, Depaiwa N, Yenwichai T, Intano W, Masomtob M. Improvement of estimation method for battery cell heat generation. Journal of Research and Applications in Mechanical Engineering. 2021;9(2):JRAME-21-9-013:1–10.

[14] Payakthong S, Pornpibul T. Steam consumption analysis on the venting process in direct steam retort. International Journal of Advancements in Mechanical and Aeronautical Engineering. 2018;5(1):148–152.
[15] Fragiacomo P, Martorelli M, Genovese M, Piraino F, Corigliano O. Thermodynamic modelling, testing and sensitive analysis of a directly pressurized hydrogen refuelling process with a compressor. Renewable Energy. 2024;226:120410.
[16] Phukapak S. Experimental study of solidification process of tubular-ice [Master's thesis]. Khon Kaen: Khon Kaen University; 2012.
[17] Stoecker WF, Jones JW. Refrigeration and air conditioning. McGraw-Hill; 1982.
[18] Arora CP. Refrigeration and air conditioning. 3rd ed. McGraw-Hill; 2009.
[19] Stephan K, Abdelsalam M. Heat-transfer correlations for natural convection boiling. International Journal of Heat and Mass Transfer. 1980;23(1):73–87.
[20] Özışık MN. Heat transfer: A basic approach. McGraw-Hill; 1985.
[21] Stoecker WF. Design of thermal systems. 3rd ed. McGraw-Hill; 1989.
[22] Moore H. MATLAB for engineers. Pearson Education; 2022.
[23] Theamtat T, Koonsrisuk A. Fluid selection and optimal operating conditions of an ORC and trilateral Rankine cycle power plant for a heat source temperature of 210°C–250°C. Journal of Research and Applications in Mechanical Engineering. 2020;8(2):135–147.
[24] Piruchvet N. A numerical study of the effect of the convective heat transfer coefficient on the production rate of tubular-ice [Master's thesis]. Bangkok: Chulalongkorn University; 2005.